BAYESIAN INFERENCE OF INTRAVOXEL STRUCTURE IN DIFFUSION MRI

Haifang Ge[1]*, William J. Fitzgerald*[1] *, and Hadrian A.L. Green*[2]

[1]Cambridge University Engineering Department
Signal Processing Laborotary
Trumpington Street
Cambridge, CB2 1PZ, UK

[2]Wolfson Brain Imaging Centre
Addenbrooke's Hospital and
Cambridge University
Cambridge, CB2 2QQ, UK

ABSTRACT

While diffusion tensor imaging (DTI) provides a powerful tool to reconstruct neural pathways in vivo, the standard diffusion tensor model is limited to resolve a single fiber direction within each voxel. To overcome this difficulty, high angular resolution diffusion imaging (HARDI) has recently been proposed to investigate intravoxel fiber heterogeneity. In this paper we propose a novel method for mixture model decomposition of the HARDI signal based on Bayesian inference and trans-dimensional Markov Chain simulation. The method is applied to both synthetic and real data.

1. INTRODUCTION

Magnetic resonance diffusion tensor imaging (DTI) assumes that the water diffusion within each voxel follows a Gaussian distribution. But in voxels containing multiple fiber tracts with different orientations this assumption no longer holds and diffusion tends to be multimodal. This is a significant limitation for DTI since at the typical image resolutions used in diffusion MRI, the volume of cerebral white matter containing such intravoxel orientational heterogeneity may be considerable [5]. Q-space imaging(QSI), or diffusion spectrum imaging (DSI) [10], and high angular resolution diffusion imaging (HARDI) [2, 9] are two methods which have recently been proposed to resolve intravoxel multiple fiber directions. In comparison, HARDI is less demanding than DSI in terms of acquisition times and magnetic field gradient, and is, therefore, more widely used.

The application of HARDI requires a reconstruction scheme which can either be model-based [2, 4, 6, 9] or model-free [11]. Here, we propose a novel mixture model based inversion method which makes use of Bayesian estimation and trans-dimensional Markov chain simulation [3, 7]. Due to experimental uncertainties present in diffusion MR imaging, Bayesian approach is believed to have potential advantages in diffusion MRI data processing [1].

2. METHODS

2.1 Mixture models for multiple-fiber structure

DTI measures the molecular diffusion of water along neural pathways. For a voxel containing a single fiber, the diffusion signal is given by [8]

$$S = S_0 e^{-b\mathbf{v}^T \mathbf{D} \mathbf{v}} \tag{1}$$

where S_0 is the signal intensity without the diffusion weighting, $\mathbf{v}$ is an unit vector defining the applied gradient direction, and $\mathbf{D}$ is the diffusion tensor which can be seen as synonymous with a "fiber". Assuming the orientation of the fiber aligns with $(\ ,\ )$ as shown in Fig.1, the diffusion tensor $\mathbf{D}$ can be parameterized as:

$$\mathbf{D} = \mathbf{R}^T \mathbf{D}\ \ \mathbf{R} \tag{2}$$

where

$$\mathbf{D} = \begin{bmatrix} {}_1 & 0 & 0 \\ 0 & {}_2 & 0 \\ 0 & 0 & {}_3 \end{bmatrix} \tag{3}$$

and $(\ {}_1,\ {}_2,\ {}_3)$ are the principle diffusivities. $\mathbf{R}$ is the rotation matrix which relates the generally unknown principle diffusion axes to the laboratory coordinate system.

$$\mathbf{R} = \begin{bmatrix} \cos\ \cos & \cos\ \sin & -\sin \\ -\sin & \cos & 0 \\ \sin\ \cos & \sin\ \sin & \cos \end{bmatrix} \tag{4}$$

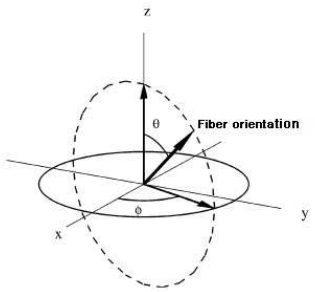

Figure 1: The fiber orientation in the laboratory coordinate system.

To model the underlying structure of a voxel with multiple fibers, we assume no diffusion exchange between fibers, i.e., the contribution of each fiber to the overall diffusion is independent and additive. This leads naturally to the diffusion signal from a voxel containing k fibers being a mixture of Eq.(1) [2, 9]

$$S = S_0 \sum_{j=1}^{k} {}_j \exp(-b\mathbf{v}^T \mathbf{D}_j \mathbf{v}) \tag{5}$$

where $\mathbf{D}_j$ is a tensor corresponding to a fiber, as defined above in Eq.(2)-(4). ${}_j$ is the fraction of signal contributed by the corresponding fiber $\left(\sum_{j=1}^{k} {}_j = 1 \right)$.

[1]hg251@cam.ac.uk, wjf@eng.cam.ac.uk
[2]halg2@wbic.cam.ac.uk

2.2 Bayesian estimation for mixture models

Given the observed diffusion weighted signal S at a voxel, our goal is to estimate the number of fibers k contained, the fiber weights $\mathbf{w} = (\ _1, \ldots, \ _k)$ and the fiber parameters $\mathbf{\Theta} = (\ _1, \ldots, \ _k)$, $\ _j = (\ _j, \ _j, \ _{1,j}, \ _{2,j}, \ _{3,j}, S_0, \ ^2)$, $j = 1, \ldots, k$. In a Bayesian framework, the posterior density is written in general as

$$p(k, \mathbf{w}, \mathbf{\Theta}|S) \quad p(k)p(\mathbf{w}|k)p(\mathbf{\Theta}|k)\,p(S|k, \mathbf{w}, \mathbf{\Theta}) \tag{6}$$

By assuming i.i.d. Gaussian noise $(0, \ ^2)$ for the diffusion MRI acquisition process, the likelihood

$$p(S|k, \mathbf{w}, \mathbf{\Theta}) = \mathbf{N}(S|\overline{S}, \ ^2) \tag{7}$$

where $\overline{S}$ is the expected diffusion signal calculated through Eq.(5). For HARDI we usually measure the diffusion signal S along many directions. Letting n be the number of measurements made, we then have the observed signal $\mathbf{S} = (S_1, \ldots, S_n)$ and the likelihood in Eq.(7) is extended to include all S_i

$$p(\mathbf{S}|k, \mathbf{w}, \mathbf{\Theta}) = \prod_{i=1}^{n} p(S_i|k, \mathbf{w}, \mathbf{\Theta}) \tag{8}$$

For priors in Eq.(6) we choose k to follow a uniform distribution $U(1, k_{\max})$, $k_{\max}$ is the pre-specified maximum number of fibers, and $\mathbf{w}$ to be a symmetric Dirichlet $D(1, \ldots, 1)$. Priors on fiber parameters $\mathbf{\Theta}$ are taken as non-informative, namely $\ _{1:k} \sim U(0, \ )$, $\ _{1:k} \sim U(-\ , \ )$, $S_0 \sim U(0, \ )$, and $\ ^{-2} \sim Gamma(\ , \ )$ to ensure positive constraints.

2.3 Reversible jump sampling

Since the number of fibers is unknown, it is desirable to carry out a trans-dimensional Markov chain simulation for solving Eq.(6), in which the dimension of the parameter space is allowed to vary. We adopt a reversible jump MCMC [3, 7] approach in our work. Our algorithm includes two move types:

- The fixed-k moves. Proposed with probability $p_F(k)$, it consists of Metropolis-Hasting proposals for each $(S_0, \ _{1:k}, \ _{1:k}, \ _{1:k}, \ _{1:k}, \ ^2)$ with independent accept/reject decisions. The proposal is a multiplicative lognormal random walk on the $\ _j$'s, $\ _j$'s and $\ ^2$'s, and an additive normal random walk on the S_0, $\ _j$'s and $\ _j$'s.
- Birth or death moves. First a random choice is made between birth and death, using the predefined probability $p_B(k)$ and $p_D(k)$. For a birth move, a new component is proposed, with its weight and parameters drawn from a joint density $J((\ _{k+1}, \ _{k+1})|k, k+1, (\mathbf{w}, \mathbf{\Theta}))$. Specifically, is drawn using $\ _{k+1} \sim Be(1, k)$, Be being the Beta distribution, and parameters $\ _{k+1}$ drawn from the prior introduced in the previous section. To make all weights sum to 1, the existing weights are rescaled by $\ _j = \ _j(1 - \ _{k+1})$, $j = 1, \ldots, k$. For a death move, each existing component is selected with equal probability, the selected component is deleted, and the remaining weights are rescaled to sum to 1. The moves are accepted with probability $\min(r, 1)$ for birth and $\min(r^{-1}, 1)$ for death, where the ration r is given by

$$\begin{aligned} r = & \frac{p(k+1, (\mathbf{w}^*, \mathbf{\Theta}^*) \cup (\ _{k+1}, \ _{k+1})|\mathbf{S})}{p(k, \mathbf{w}, \mathbf{\Theta}|\mathbf{S})} \\ & \times \frac{p_D(k+1)/(k+1)}{p_B(k)J((\ _{k+1}, \ _{k+1})|k, k+1, (\mathbf{w}, \mathbf{\Theta}))} \\ & \times \left| \frac{\left(g_{k,k+1}((\mathbf{w}, \mathbf{\Theta}) \cup (\ _{k+1}, \ _{k+1}))\right)}{((\mathbf{w}, \mathbf{\Theta}) \cup (\ _{k+1}, \ _{k+1}))} \right| \end{aligned} \tag{9}$$

where the last term is a Jacobian arising from the change of variable, $(\mathbf{w}^*, \mathbf{\Theta}^*) \cup (\ _{k+1}, \ _{k+1}) = g_{k,k+1}((\mathbf{w}, \mathbf{\Theta}) \cup (\ _{k+1}, \ _{k+1}))$ and $\dim((\mathbf{w}, \mathbf{\Theta})) + \dim((\ _{k+1}, \ _{k+1})) = \dim((\mathbf{w}^*, \mathbf{\Theta}^*) \cup (\ _{k+1}, \ _{k+1}))$, which do the dimension matching to ensure the detailed balance condition of the Markov chain. Through the carefully chosen proposal distribution, the above equation can be written in a simple form

$$r = \frac{p(\mathbf{S}|k+1, (\mathbf{w}, \mathbf{\Theta}) \cup (\ _{k+1}, \ _{k+1}))\, p_D(k+1)}{p(\mathbf{S}|k, \mathbf{w}, \mathbf{\Theta})\, p_B(k)} \tag{10}$$

2.4 Data acquisition

Diffusion weighted images were acquired along 60 directions equally spaced on a sphere by tessellations of an icosahedron, with a b-value$\approx$ 1000mm^2/s, along with 4 images acquired at $b \approx 0$. The imaging parameters were: slice thickness = 2.3mm, FOV = 190×190mm^2, matrix size 100×100. Images were reconstructed on a 128×128 matrix giving a final resolution of $1.5 \times 1.5 \times 2.3$mm^3, TR = 2.2s, TE = 105ms. Imaging was implemented on a 3.0-T clinical whole body magnet (Bruker Medspec s300; Bruker Medical) using a echo-planar imaging technique. The local research ethics committee approved the study.

3. RESULTS

3.1 Verification of the method

The estimation procedure was tested on simulated HARDI data. The test is conducted as follows. First, 60-direction measurements of HARDI with given parameters (true parameters) is generated by a simulator. These measurements serve as the data for the estimation procedure. Then the estimated parameters (posterior mean) are compared to the true parameters. The mean minimum angle difference (MMAD) [9] was calculated as the comparison index

$$\text{MMAD} = \frac{1}{k} \sum_{j=1}^{k} \min\left(\cos^{-1}(\hat{\mathbf{e}}_j \cdot \mathbf{e}_i)\right) \quad \text{for} \quad i = 1, \ldots, k \tag{11}$$

where k is the number of fibers, $\hat{\mathbf{e}}_j$ is the estimated orientation of the jth fiber, and $\mathbf{e}_i$ is the true fiber orientation. Figure 2 shows the estimation results for two fiber mixtures, the example taken from [9]. Both fiber have the same principle diffusivities $(\ _1, \ _2, \ _3) = (1.7, 0.3, 0.3)$ m^2/ms, and is separated by an increasing angle from 0° to 90°. The estimation procedure was run 20 times for each angular separation. The attenuated SNR level was set at 25 assuming Gaussian noise.

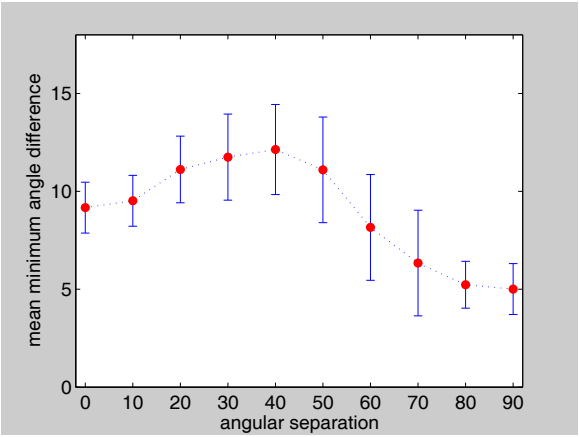

Figure 2: Accuracy (mean $\pm$ standard deviation) of 2-fiber mixture analysis.

3.2 Application on human brain data

The first region chosen to do Bayesian mixture analysis is shown in Figure 3 (left) bounded by a white box. It is an area where the mediolaterial corpus callosum intersects with superoinferior corona radiata [12]. The inferred introvoxel structure is visualized using color-coded and anisotropy scaled cylinders (right). Each cylinder represents a fiber population within the voxel. For comparison, the DTI map of the same area is also shown in the middle. It can be seen that Bayesian mixture analysis reveals the fiber crossing between the corona radiata (blue) and radiation of the corpus callosum (red) while DTI only shows an averaging of fibers within the voxel.

Another region of interest (Figure 4, right) has more complex neural architecture [11]. The area selected covers the partial neural circuit between the prefrontal cortex and the mediodorsal nucleus of the thalamus, containing both intersection and dispersion of fibers. Starting from the internal capsule, the fiber has an anteroposterior orientation. It intersects the mediolateral-directed genu of the corpus callosum, and diverges into the inferior frontal gyrus, the middle frontal gyrus and the superior frontal gyrus. Bayesian analysis of the mixture model reveals the fiber crossing with the corpus callosum. But due to artefacts in the middle, the fiber dispersion area was only partially imaged and estimation for both single tensor DTI and mixtures affected. It shows only partially that fibers diverge laterally into the inferior frontal gyrus, and shows some signs of fiber dispersion into middle and superior frontal gyrus. Again, the DTI single tensor model fails to identify voxels containing multiple fiber populations.

4. DISCUSSION

In [1] a Bayesian approach was proposed to estimate parameters defining local fiber direction, but the estimation process was limited to the case where only a single fiber orientation is modeled in each voxel. We extend [1] by using a novel Bayesian analysis to include multiple fibers within a voxel, which enables us to set up a fully probabilistic framework to infer anatomical connectivity in the human brain.

ACKNOWLEDGMENTS

The authors, in particular Haifang Ge, would like to thank Dr. G.Parker at University of Manchester for helpful discussions on the mixture models.

REFERENCES

[1] T. E. J. Behrens, M. W. Woolrich, M. Jenkinson, H. Johansen-Berg, R. G. Nunes, S. Clare, P. M. Matthews, J. M. Brady and S. M. Smith, "Characterization and propagation of uncertainty in diffusion weighted MR imaging," *Magnetic Resonance in Medicine*, vol. 50, pp. 1077–1088, 2003.

[2] L. R. Frank, "Characterization of anisotropy in high angular resolution diffusion-weighted MRI," *Magnetic Resonance in Medicine*, vol. 47, pp. 1083–1099, 2002.

[3] P. J. Green, "Reversible jump Markov chain Monte Carlo computation and Bayesian model determination," *Biometrika*, vol. 82, pp. 711–732, 1995.

[4] K. M. Jansons and D. C. Alexander, "Persistent angular structure: new insights from diffusion magnetic resonance imaging data, " *Inverse Problems*, vol. 19, pp. 1031–1046, 2003.

[5] J. M. Meyer, N. Makris, J. F. Bates, V. S. Caviness and D. N. Kennedy, "MRI-Based topographic parcellation of human cerebral white matter," *Neuroimage*, vol. 9(1), pp. 1–17, Jan., 1999.

[6] E. Ozarslan and T. H. Mareci, "Generalized diffusion tensor imaging and analytical relationships between diffusion tensor imaging and high angular resolution diffusion imaging, " *Magnetic Resonance in Medicine*, vol. 50, pp. 955–965, 2003.

[7] S. Richardson and P. J. Green, "On Bayesian analysis of mixtures with an unknown number of components (with discussion)," *Journal of Royal Statistics Society*, **B**59, pp. 731–792, 1997.

[8] E. O. Stejskal and J. E. Tanner, "Spin diffusion measurements: spin echos in the presence of a time-dependent field gradient," *Journal of Chemical Physics*, vol. 42, pp. 288–292, 1965.

[9] D. S. Tuch, T. G. Reese, M. R. Wiegell, N. Makris, J. W. Belliveau and J. Van Wedeen, "High angular resolution diffusion imaging reveals intravoxel white matter fiber heterogeneity," *Magnetic Resonance in Medicine*, vol. 48, pp. 577–582, 2002.

[10] D. S. Tuch, *Diffusion MRI of complex tissue structure[Doctoral dissertation]*. Cambridge, Massachusetts: Harvard University-MIT, 2002. 218p.

[11] D. S. Tuch, "Q-Ball imaging, " *Magnetic Resonance in Medicine*, vol. 52, pp. 1358–1372, 2004.

[12] M. R. Wiegell, H BW Larsson, Dr med and Van J. Wedeen, "Fiber Crossing in Human Brain Depicted with Diffusion Tensor MR Imaging," *Radiology*, vol. 217, pp. 897-903, 2000.

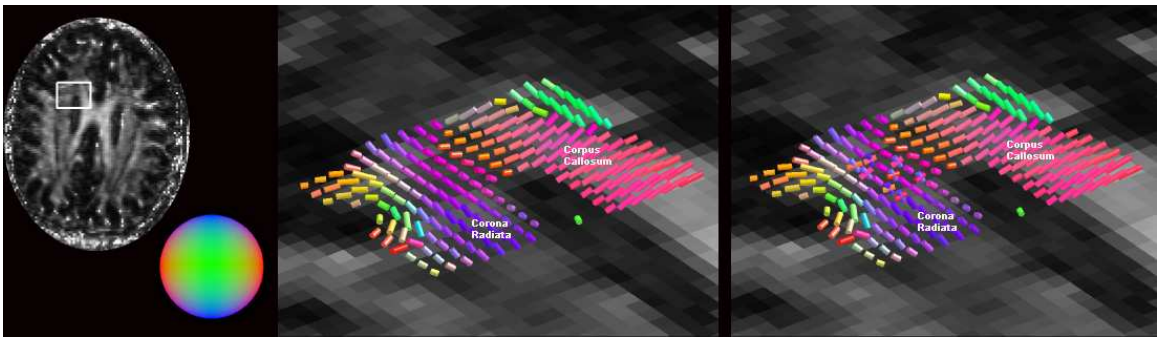

Figure 3: Left: Transverse view of the fractional anisotropy image showing the ROI. The region includes the crossing between the coronal radiator and radiation of the corpus callosum. Middle: Single tensor reconstruction of DTI. The tensor at each voxel represents a fiber population and is visualized with a cylinder oriented in the direction of the first eigenvector, scaled by the fractional anisotropy, and color coded according to the RGB sphere shown at left, with red indicating mediolateral, green anteroposterior, and blue superoinferior. Right: Bayesian mixture analysis of HARDI signal rendered by multi-cylinder. The orientations of the cylinders are determined by posterior mean estimation of (,) and color cloded using the same scheme. Fiber crossing can be seen at intersection of the corpus callosum with the coronal radiator.

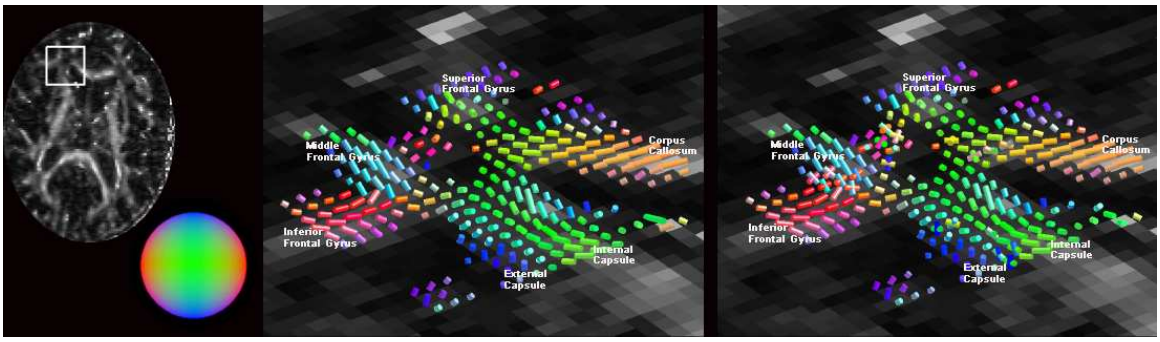

Figure 4: Left: Transverse view of the fractional anisotropy image showing the ROI bounded in the white box. Middle and right: Rendering of the DTI map and the recovered multi-fiber field using the same methods as described in Figure 3. The Bayesian analysis of mixture model infers the crossing between callosal genu fibers and the fibers passing through the internal capsule; and the intersection of fibers from the external capsule with the uncinate fascicle. Also, the dispersion of fibers into the frontal gyri can be partially seen.